# Microbial Degradation of Heptenophos in the Soil Environment by Biological Baeyer–Villiger Oxidation

Wilfried Schwab,* Petra Dambach, and Harald J. Buhl

Hoechst AG, 65926 Frankfurt am Main, Germany

The transformation of 0.67 μg/g [6-$^{14}$C]heptenophos was investigated, under laboratory conditions, in a microbiologically active soil and an autoclaved soil at 40% of their maximum water holding capacity and at 20 °C. Over a 240-h period in active and sterile soil, 22% and 0% of the applied $^{14}$C was released as carbon dioxide, whereas 41% and 93% of the initial radioactivity was solvent recoverable, respectively. Three principal and four minor metabolites were detected by reversed-phase high-performance liquid chromatography in biologically active soil. Major metabolites were separated and characterized by gas chromatography/Fourier transformation infrared spectroscopy and gas chromatography/mass spectral techniques. For the first time, two major metabolites were identified as 3-chloro-3,3a,6,6a-tetrahydro-2*H*-cyclopenta[*b*]furan-2-one and 3,3a,6,6a-tetrahydro-1*H*-cyclopenta[*c*]furan-1-one, whereas the third principal transformation product was tentatively characterized as (5-oxo-2-cyclopentenylidenyl)ethanoic acid. Hydrolysis product 7-chlorobicyclo[3.2.0]hept-2-en-6-one was a minor metabolite. Degradation products 3-chloro-3,3a,6,6a-tetrahydro-2*H*-cyclopenta[*b*]furan-2-one and 3,3a,6,6a-tetrahydro-1*H*-cyclopenta[*c*]furan-1-one appear to be the first pesticide metabolites formed by biological Baeyer–Villiger oxidation. In autoclaved soil, 7-chlorobicyclo[3.2.0]hept-2-en-6-one and 3-chloro-3,3a,6,6a-tetrahydro-2*H*-cyclopenta[*b*]furan-2-one were detected after 168 h of incubation.

**Keywords:** *Heptenophos, microbial degradation, soil, Baeyer–Villiger oxidation, pesticide, metabolism*

## INTRODUCTION

Heptenophos (7-chlorobicyclo[3.2.0]hepta-2,6-dien-6-yl dimethyl phosphate) is the active ingredient in the Hoechst insecticide Hostaquick and has been used since 1970 for the control of parasitic insects and mites (Hewson, 1975; Bonin, 1975). It is applied to crops at a maximum recommended field rate of 500 g of active ingredient/ha. Field research and laboratory research on bioefficacy and degradation of heptenophos indicate its short persistence in soil (Emmel et al., 1970). The half-life of heptenophos ranges from 1 to 25 h. Because of the very short persistence of heptenophos, the potential either to develop high residue levels in soil or crops or to leach is minimal. Although the rapid disappearance of heptenophos in soils has been well documented, little is known about the mechanism of degradation or the factors influencing its degradation.

In the present study, the metabolism of the active ingredient heptenophos was investigated in microbially active and autoclaved soil. The objectives were to identify transformation products and to clarify the role of microorganisms in the rapid degradation process. Rate, type, and degree of metabolism of the pesticide and its major degradation products were determined.

## EXPERIMENTAL PROCEDURES

**Soils.** The soil was collected to a depth of 0–15 cm from a test field south of the company's ground in April 1992. The soil properties are as follows: texture, sandy loam, pH 5.70; organic matter, 1.87%; organic carbon, 1.09%; maximum water holding capacity, 32.11%; microbial biomass, 38.00 mg of C/100 g; cation-exchange capacity, 6.21 mval/100 g; density, 1.16 g/cm$^3$; clay, 9.51%; silt, 36.60%; sand, 53.88%. The test field had not been treated with heptenophos during the previous 5 years. Shortly before the study was started, the soil was sieved through a 2-mm sieve, moistened with distilled water to 40% of its maximum water holding capacity, and kept in darkness for an acclimatization period of 1 week (20 ± 2 °C). During this period, distilled water was added to maintain the original water content. This procedure was in coincidence with the guideline of Biologische Bundesanstalt, Germany, *Fate of Plant Protection Products in Soil – Degradation, Conversion and Metabolism.* To allow comparison of microbial and chemical degradation, a portion of the field-collected soil was autoclaved at 124 °C and 1.25 bar for 30 min. The autoclaved soil was prepared in the same way as the fresh field soil.

**Table 1. Number References to Compounds**

| no./compd | nomenclature |
|---|---|
| | Active Ingredient and Formed Metabolites |
| heptenophos | 7-chlorobicyclo[3.2.0]hepta-2,6-dien-6-yl dimethyl phosphate |
| 1 | 7-chlorobicyclo[3.2.0]hept-2-en-6-one |
| 2 | 3-chloro-3,3a,6,6a-tetrahydro-2*H*-cyclopenta[*b*]-furan-2-one |
| 3 | unknown metabolite |
| 4 | 3,3a,6,6a-tetrahydro-1*H*-cyclopenta[*c*]furan-1-one |
| 5 | (5-oxo-2-cyclopentenylidenyl)ethanoic acid (tentatively identified) |
| 6 | unknown metabolite |
| 7 | unknown metabolite |
| | Reference Compounds and Postulated Intermediates |
| 8 | 3-chloro-3,3a,6,6a-tetrahydro-1*H*-cyclopenta[*c*]-furan-1-one |
| 9 | (±)-bicyclo[3.2.0]hept-2-en-6-one |
| 10 | 3,3a,6,6a-tetrahydro-2*H*-cyclopenta[*b*]furan-2-one |

**Chemicals.** [6-$^{14}$C]Heptenophos (7-chlorobicyclo[3.2.0]hepta-2,6-dien-6-yl dimethyl phosphate) (Table 1), specific radioactivity 1.467 MBq/mg (0.040 mCi/mg), radiochemical purity >98%, was obtained from the Radiochemical Laboratory of Hoechst AG. Analytical grade heptenophos (95%) and metabolite standard 7-chlorobicyclo[3.2.0]hept-2-en-6-one (1) (98%) were obtained from the Product Analysis Unit, Hoechst AG. (±)-Bicyclo[3.2.0]hept-2-en-6-one (9) and 3,3a,6,6a-tetrahydro-2*H*-cyclopenta[*b*]furan-2-one (10) (Corey lactone) were purchased from Merck-Schuchardt, Germany, and Aldrich, Germany, respectively.

**Soil Treatment.** After the acclimatization period, duplicate samples (50 g) of biologically active and autoclaved soil at 40% of their maximum water holding capacity were weighed into 300-mL Erlenmeyer flasks and treated with 33.7 μg of radiolabeled heptenophos. Glass tubes (length 15 cm) were placed on top of the Erlenmeyer flasks. These tubes contained two layers of soda

0021-8561/94/1442-1578$04.50/0 

lime granules separated by glass wool. The soda lime layer at the top prevented entry of atmospheric $CO_2$, whereas the layer beneath served as absorption trap for $^{14}CO_2$ formed by mineralization. The bottom of the tube was closed with glass wool coated with viscous paraffin. This layer absorbed volatile organic transformation products.

**Recovery and Extraction of Radioactivity.** At each sampling date, the batches were analyzed for (a) radioactive content of soil extract and extracted soil, (b) amount of volatiles, (c) overall recovery, and (d) identity of the extractable radioactive residues. Soil samples were extracted at least three times with 100-mL aliquots of a solvent mixture composed of acetonitrile/water (4:1 v/v). Extracts were examined for radioactivity by liquid scintillation counting (LSC). Radioactivity which persisted in the soil following solvent extraction was determined by combustion and subsequent measurement of evolved $^{14}CO_2$. Absorption tubes for volatile organic metabolites and $^{14}CO_2$ formed by mineralization were worked up as follows: The upper layer of soda lime in each absorption tube and the glass wool underneath were discarded, after which the lower layer of soda lime was filled into an Erlenmeyer flask and analyzed for $^{14}CO_2$. $^{14}CO_2$ was liberated after addition of 50 mL of HCl (18%) and trapped in 10-mL of Carbosorb which was finally measured by LSC. The glass wool at the bottom of the absorption tubes was soaked in 10 mL of diethyl ether. This extract was also analyzed by LSC.

**Metabolite HPLC Analysis.** The degradation of heptenophos and its transformation products was monitored using high-performance liquid chromatography (HPLC). The HPLC equipment consisted of a Spectra Physics SP 8780 HPLC equipped with a Spectroflow 757 UV–visible absorbance detector (Kratos) set at 230 nm and a Ramona 5 radioactivity monitor (Raytest) with a 200-$\mu$L detector cell filled with solid scintillator. The HPLC was fitted with an ODS Hypersil column (25 cm × 4.0 mm i.d., particle size 5 $\mu$m). The profiling HPLC gradient was conducted in a linear step at a flow rate of 1 mL/min, utilizing acetonitrile and acidic water, adjusted to pH 2.5 with 1.0 M sulfuric acid. The gradient proceeded form 0% to 100% acetonitrile in 30 min and remained at 100% acetonitrile for an additional 10 min.

**Metabolite HPLC Isolation.** Metabolites **1**, **2**, **4**, and **5** were isolated by semipreparative HPLC of combined metabolism samples of hour 8 to hour 240, using the same conditions as described for HPLC metabolite profiling. Acetonitrile in the collected fractions was removed by rotary evaporation, and the transformation products were extracted with diethyl ether. After concentration under reduced pressure, the isolates were analyzed by GC/MS and GC/FTIR. In the case of transformation product **5**, the following methylation procedure was performed prior to GC/MS and GC/FTIR analysis.

**Methylation Procedure.** An aliquot (25 $\mu$L) of a (trimethylsilyl)diazomethane solution in hexane (2.0 M) (Aldrich) was added to the chilled diethyl ether solution (1 mL) of transformation product **5**. The reaction mixture was allowed to warm to room temperature and kept in a hood for 1 day. The solution was washed successively with saturated sodium hydrogen carbonate solution and water and dried over sodium sulfate. Diethyl ether was partly removed by a stream of nitrogen.

**Liquid Scintillation Counting Analysis (LSC).** Aliquots of liquid samples were added to 10 mL of scintillation cocktail Rotiszint eco plus (Roth). Solid samples were combusted in a biological oxidizer (Model Ox 500; Zinsser Analytic). The formed $^{14}CO_2$ was absorbed in 12 mL of Oxysolve 400 (Zinsser Analytic). Recoveries of $^{14}C$ as [$^{14}C$]carbon dioxide from test combustions fortified with $^{14}C$ standards, immediately before combustion, were greater than 95%. All measurements were carried out by means of the liquid scintillation counter TRI-CARB 4530 (Packard Instruments) after decaying of the chemiluminescence counts.

**Gas Chromatography/Mass Spectroscopy (GC/MS).** GC/MS analyses were performed on FUSI DB1 capillary columns (30 m long × 0.32 mm i.d., film thickness 0.25 $\mu$m), using a GC 8000 (CE/FISON Instruments) equipped with a TRIO 2000 mass spectrometer (VG/FISONS Instruments) and an initial program temperature of 60 °C (0 min) followed by an increase to 300 °C at 10 °C/min. Electron impact (EI) and chemical ionization (CI) spectra using ammonia as the reagent gas were obtained.

**Gas Chromatography/Fourier Transformation Infrared Spectroscopy (GC/FTIR).** GC/FTIR analyses were performed on RTX-1 capillary columns (30 m long × 0.32 mm i.d., film thickness 0.5 $\mu$m), using an HP 5890 Series II gas chromatograph (Hewlett-Packard) linked to a Bruker IFS 88 FTIR spectrometer and an initial temperature of 60 °C (0 min) followed by an increase to 300 °C at 10 °C/min. The light pipe was heated to 280 °C.

**Nuclear Magnetic Resonance Spectroscopy (NMR).** $^1H$ and $^{13}C$ NMR spectra were obtained using a Varian VXR 5000 (300-MHz) instrument.

**Synthesis of 3-Chloro-3,3a,6,6a-tetrahydro-2*H*-cyclopenta[*b*]furan-2-one (2) (Baeyer–Villiger Oxidation).** Ketone **1** (5.00 g, 35.0 mmol) and potassium hydrogen sulfate (0.16 g, 1.9 mmol) were added to 50 mL of methanol. The reaction mixture was stirred at room temperature until all of the salt had dissolved, and hydrogen peroxide (1.43 g, 42.1 mmol) was added carefully. During this exothermal process, the reaction mixture was allowed to warm to 50 °C. After 1 day, 50 mL of an aqueous sodium thiosulfate solution (13.0 g, 48 mmol) was added and the solution was stirred for 10 min. This mixture was poured into 50 mL of water and extracted three times with dichloromethane. The dichloromethane extract was dried over sodium sulfate, concentrated by rotary evaporation, and fractionated on a silica gel column using ethyl acetate/petroleum ether (3:7 v/v) as eluent. Two isomers (**2** and **8**) were obtained. **2** was characterized by the following data: EI-MS (70 eV) *m/z* (%) 79 (100), 77 (29), 65 (15), 78 (8), 51 (7), 158 [$M^+$, $^{35}Cl$] (6), 95 (4), 101 (3), 160 [$M^+$, $^{37}Cl$] (2), 103 (1), 113 (1); $^1H$ NMR (300 MHz, $CDCl_3$) $\delta$ 2.8 (2 H, m, $CH_2$), 3.8 (1 H, m, CH-CHCl), 4.78 (1 H, d, CHCl), 5.11 (1 H, m, CH-O), 5.81 and 5.93 (2 × 1 H, m, 2 CH=); $^{13}C$ NMR (300 MHz, $CDCl_3$) $\delta$ 42.6 ($CH_2$-), 53.6 and 56.9 (2 CH-), 83.1 (CH-Cl), 129.2 and 134.0 (2 CH=), 173.7 (C=O).

**Synthesis of 3,3a,6,6a-Tetrahydro-1*H*-cyclopenta[*c*]furan-1-one (4) (Baeyer–Villiger Oxidation).** Lactone **4** was synthesized analogously to lactone **2**, except that ketone **9** was used as starting material instead of **1**. Two isomers (**4** and Corey lactone **10**) were obtained. **4** was characterized by the following data: EI-MS (70 eV) *m/z* (%) 66 (100), 79 (36), 65 (7), 96 (5), 123 (4), 67 (4), 124 [$M^+$] (3), 94 (2), 77 (5), 97 (4).

## RESULTS

**Recovery and Extraction of Radioactivity.** The recovery data for the different fractions at all sampling times are shown as percentages of applied radioactivity in Table 2. The total recovery at all sampling times during the course of the study ranged from 86.9% to 102.1% of applied radioactivity (mean values). The $^{14}CO_2$ production accounted for 21.9% of applied radioactivity (mean value) after 240 h of incubation for the biologically active soil. Determination of $^{14}CO_2$ production in the autoclaved soil samples was not performed. Since total applied radioactivity was recovered in the autoclaved soil samples (data not shown), generation of $^{14}CO_2$ was excluded. Other volatiles never exceeded more than 0.1% of applied radioactivity. During the course of the study, the extractability constantly decreased and finally accounted for 41.4% (active soil) of the applied radioactivity. As a consequence, the nonextractable residues increased to 23.6%. Extractability of radioactivity in the autoclaved soil decreased only from 97.9% to 92.6% of applied radioactivity, whereas the nonextractable residues increased from 1.7% to 6.3% of applied radioactivity.

**Identification of Heptenophos Metabolites.** Analyses of the extractable radioactive residue were done by HPLC. The amount of metabolites formed during the course of the study is given for the biologically active soil in Table 3. A representative HPLC analysis of sampling date hour 49 is shown in Figure 1. Up to seven radioactive products were detected in addition to heptenophos in biologically active soil, whereas only two transformation products were formed in autoclaved soil (data not shown). Metabolite **1** was identified as 7-chlorobicyclo[3.2.0]hept-

**Table 2. Distribution of Recovered Radioactivity in Different Fractions at Various Sampling Times (Biologically Active Soil)**

| hours after application | series | extracted radioactivity (%)[a] | nonextracted radioactivity (%) | $CO_2$ (%) | volatiles (%) | recovery (%) |
|---|---|---|---|---|---|---|
| 0 | average | 99.2 | 1.6 | ND[b] | ND | 100.8 |
| 2 | average | 92.9 | 2.8 | 0.3 | 0.1 | 96.1 |
| 4 | average | 92.6 | 4.5 | 1.0 | 0.1 | 98.1 |
| 8 | average | 88.9 | 5.7 | 2.2 | 0.1 | 96.9 |
| 24 | average | 75.6 | 12.1 | 7.9 | 0.1 | 95.7 |
| 32 | average | 76.2 | 11.0 | 8.7 | 0.1 | 95.9 |
| 49 | average | 67.4 | 15.8 | 13.1 | 0.1 | 96.4 |
| 72 | average | 61.5 | 17.4 | 16.4 | 0.1 | 95.4 |
| 168 | average | 51.9 | 21.1 | 29.0 | 0.1 | 102.1 |
| 240 | average | 41.4 | 23.6 | 21.9 | 0.0 | 86.9 |

[a] Percent of applied radioactivity. [b] Not determined.

**Table 3. Percent [$^{14}$C]Heptenophos Remaining and Formation of Heptenophos Metabolites (Biologically Active Soil)**

| | | | metabolites | | | | | | | |
|---|---|---|---|---|---|---|---|---|---|---|
| hours after application | series | ai[a] 24 min[b] (%)[c] | 1, 23 min (%) | 2, 20 min (%) | 3, 18 min (%) | 4, 17 min (%) | 5, 16 min (%) | 6, 14 min (%) | 7, 3 min (%) | total (%) |
| 0 | average | 97.2 | | 2.0 | | | | | | 99.2 |
| 2 | average | 77.1 | 3.9 | 2.9 | | 6.1 | 2.9 | | | 92.9 |
| 4 | average | 73.8 | 6.4 | 5.0 | | 3.7 | 3.7 | | | 92.6 |
| 8 | average | 54.0 | 9.0 | 10.8 | | 8.9 | 6.2 | | | 88.9 |
| 24 | average | 16.9 | 2.9 | 20.4 | | 21.0 | 12.8 | 1.6 | | 75.6 |
| 32 | average | 12.8 | 2.1 | 19.6 | 1.5 | 23.7 | 14.3 | 2.2 | | 76.2 |
| 49 | average | 4.3 | 0.4 | 18.8 | 0.7 | 27.5 | 14.3 | 1.4 | | 67.4 |
| 72 | average | 2.0 | | 13.7 | 2.2 | 26.7 | 14.0 | 1.3 | 1.6 | 61.5 |
| 168 | average | 1.0 | | 3.2 | 2.3 | 28.5 | 16.2 | | 0.7 | 51.9 |
| 240 | average | 0.7 | | | 1.6 | 25.9 | 12.5 | | 0.7 | 41.4 |

[a] Active ingredient heptenophos. [b] Approximate HPLC retention time. [c] Percent of applied radioactivity.

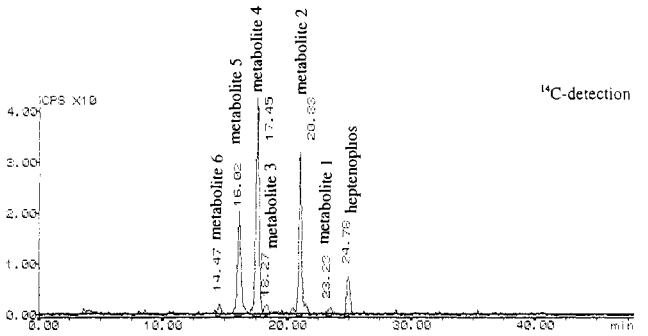


**Figure 1.** HPLC elution profile of the extracted metabolites formed from [$^{14}$C]heptenophos in biologically active soil after 49 h.

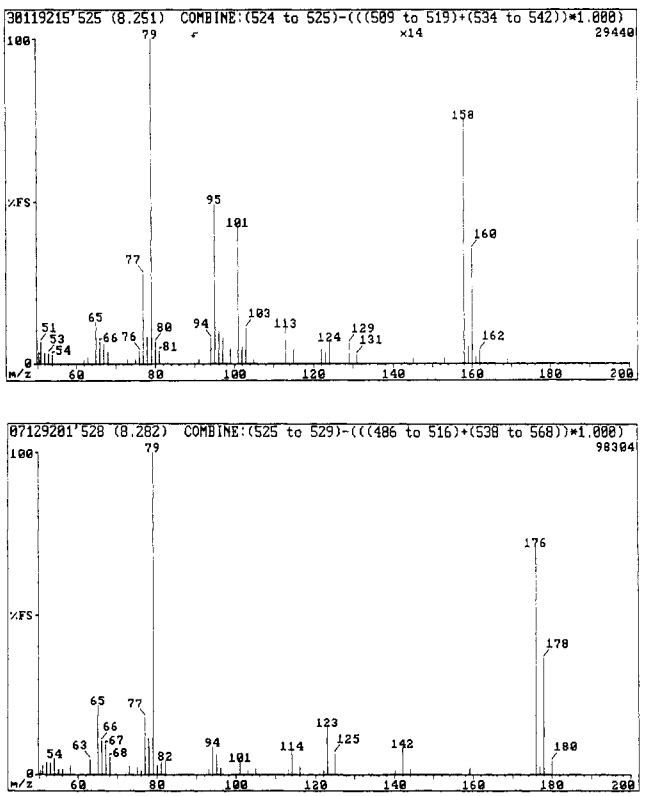


**Figure 2.** Electron impact mass spectrum of metabolite 2 (top) and chemical ionization mass spectrum (reactant gas ammonia) of metabolite 2 (bottom).

2-en-6-one by comparison of the HPLC relative retention time with those of the reference substance and by GC/MS analysis. The three principal compounds, metabolites **2**, **4**, and **5**, were isolated by semipreparative HPLC and analyzed by GC/MS. Pretests with neutral (pH 7) HPLC solvents showed that metabolite **5** is eluted with the void volume of the RP18 column. However, when an acidic (pH 2.5) HPLC solvent was used, metabolite **5** displayed a retention time of approximately 16 min. It was therefore assumed that a carboxylic group was present in the molecule, and methylation was performed prior to GC/MS analysis.

**Metabolite 2.** The EI mass spectrum obtained by GC/MS analysis of HPLC-purified metabolite 2 indicated a molecular weight of 158 (Figure 2). The ion cluster based on *m/z* 158 showed an isotope ion ratio suggesting one chlorine atom. This finding was confirmed by the corresponding CI mass spectrum displaying an $[M + NH_4]^+$ ion at 176 (Figure 2). The mass difference of the molecular weight ion of metabolite 1 and metabolite 2 is 16. Hence, the insertion of an oxygen atom into the molecule of metabolite 1 was assumed. The FTIR spectrum obtained by GC/FTIR analysis of HPLC-purified metabolite 2 (Figure 3) showed no absorption for a hydroxy group but displayed strong absorption at 1825 and 1145 $cm^{-1}$, indicating the presence of a five-membered lactone ring. Thus, structure **2** or **8** was suggested for metabolite 2. Modified Baeyer–Villiger oxidation (Matsumoto and Kobayashi, 1986) of compound **1** yielded both isomers **2**

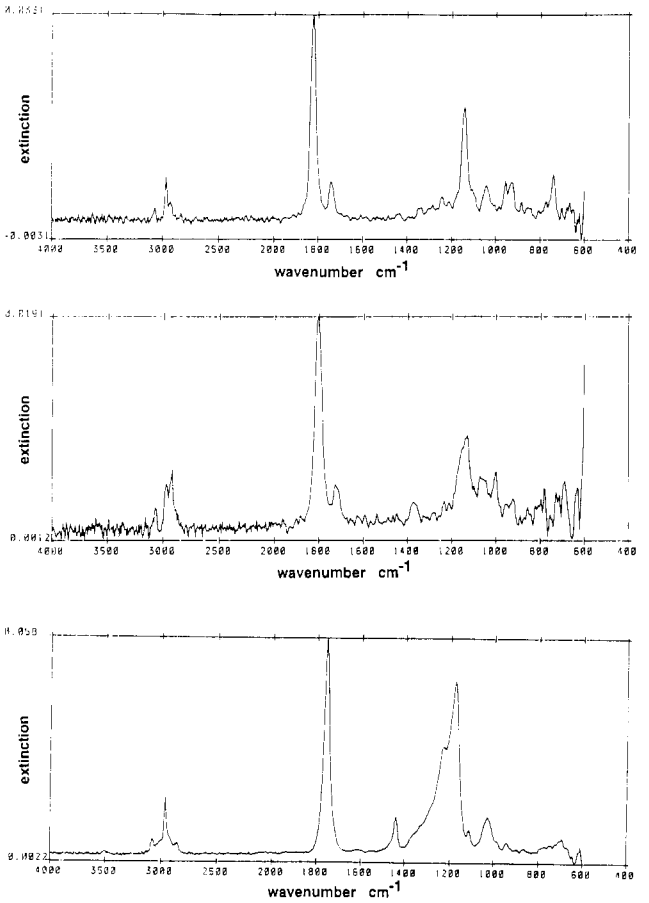


**Figure 3.** FTIR spectra of metabolite **2** (top), metabolite **4** (middle), and methylated metabolite **5** (bottom).

and **8** which were characterized by means of GC/MS and NMR analyses. Only synthetic **2** displayed properties identical with those of metabolite **2**.

**Metabolite 4.** Figure 4 shows the EI and CI mass spectra obtained by GC/MS analysis of HPLC-purified metabolite **4**. Metabolite **4** exhibited a molecular weight ion at $m/z$ 124, which was confirmed by the $[M + NH_4]^+$ ion of the CI mass spectrum at $m/z$ 142. The mass spectra also showed that a chlorine atom was not present. The FTIR spectra of **2** and metabolite **4** were almost identical (Figure 3); thus structure **4** or **10** was assumed for metabolite **4**. Compounds **4** and **10** were synthesized by Baeyer–Villiger oxidation of compound **9** according to a modified method published by Matsumoto and Kobayashi (1986). Identification of the isomers **4** and **10** was performed by comparison of the mass spectral data of the products with those of published data (Matsumoto and Kobayashi, 1986) and the commercially available reference compound **10**. Surprisingly, metabolite **4** was unambiguously identified as structure **4**.

**Metabolite 5.** EI mass spectra of methylated metabolite **5** (Figure 5) indicated a molecular weight ion at $m/z$ 152. Fragment ions at $m/z$ 59 $[OCOCH_3]^+$ and $m/z$ 93 $[m/z$ 124–$OCH_3]^+$ showed the presence of a methyl ester group, whereas a chlorine atom was missing. The FTIR spectrum obtained by GC/FTIR analysis (Figure 3) displayed a strong, broad absorption at 1755 $cm^{-1}$, indicating an ester group and/or a five-membered ketone ring. An aldehyde group was ruled out, as no absorption at approximately 2800 $cm^{-1}$ was observed. Due to the shoulder at 3000 $cm^{-1}$, a second double bond in the molecule was possible. On the basis of the EI mass spectrum and FTIR spectrum of methylated metabolite **5**, the structure for underivatized metabolite **5** shown in Figure 6 was suggested. Identification of metabolite **5** is tentative, as chemical synthesis of the proposed structure failed up to now.

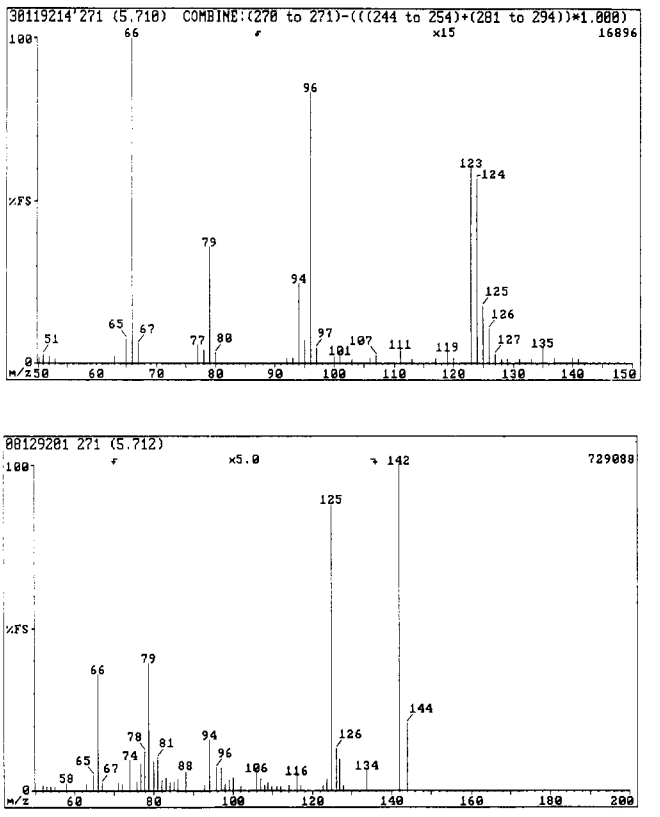


**Figure 4.** Electron impact mass spectrum of metabolite **4** (top) and chemical ionization mass spectrum (reactant gas ammonia) of metabolite **4** (bottom).

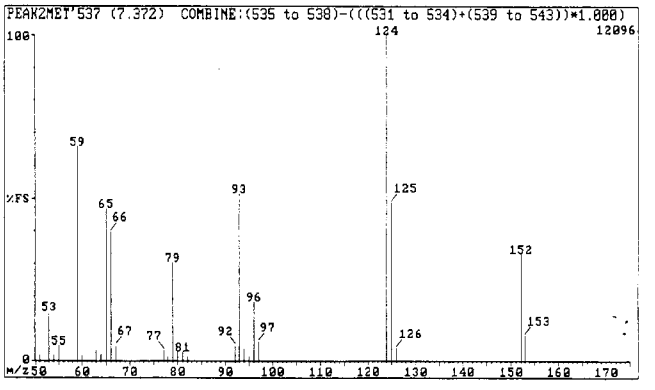


**Figure 5.** Electron impact mass spectrum of methylated metabolite **5**.

**Kinetics of Heptenophos and Metabolite Formation.** The rates of the disappearance of heptenophos and the production of metabolites **1**–**7** during 240 h of incubation are illustrated in Table 3. Corresponding data for replicates did not differ by more than 3%. Heptenophos residue data were analyzed by the method of Timme and Frehse (1980), and the method Timme et al. (1986) was used to characterize the kinetics of degradation. Best results according to the least-squares method were obtained by assuming root first-order kinetics for the biologically active soil and first-order kinetics for the autoclaved soil. DT-50 (time until 50% of the initial concentration of the test substance is degraded) and DT-90 (time until 90% of the initial concentration of the test substance is degraded) values of 3.6 and 40.3 h were calculated for the active soil, respectively, whereas DT-50 and DT-90 values of 831.6 and 2762.4 h were obtained for the autoclaved soil, respectively. Graphical evaluation of

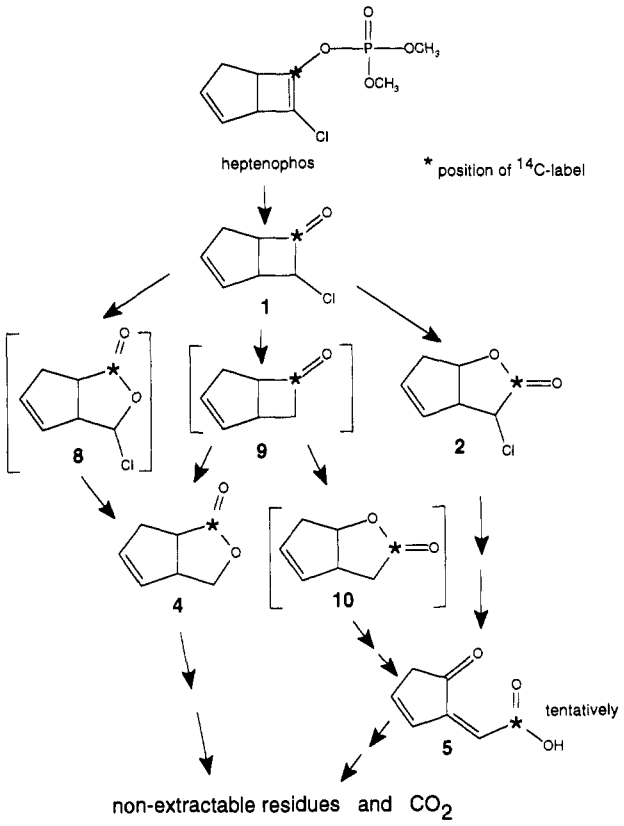


**Figure 6.** Proposed degradation pathway of heptenophos in soil.

data from Table 3 suggests DT-50 and DT-90 values of approximately 9 and 38 h, respectively. Although DT-90 values of the regression analysis and graphical evaluation are very similar, DT-50 values differ significantly. This can be explained by the relatively large deviation of the experimental data points from the regression curve at the early sampling times. The principal metabolites 4 and 5 accumulated to maximum levels at 168 h of incubation in biologically active soil, accounting for about 29% and 16%, respectively, of the applied radioactivity. However, metabolite 2 peaked at 24 h (20% of applied radioactivity). Metabolite 1 reached a maximum level at 8 h (9% of applied radioactivity). Minor metabolites 3, 6, and 7 never exceeded 2.3% of applied radioactivity and thus remained unidentified. Table 3 shows that data for heptenophos degradation in biologically active soil were collected until patterns of decline of the test substance and patterns of formation and decline of degradation products were established. In autoclaved soil, metabolites 1 and 2 were detected after 168 h of incubation (data not shown).

## DISCUSSION

The degradation of heptenophos was studied in a fresh field soil (sandy loam) and an autoclaved soil at 20 ± 2 °C. The application rates of 0.67 mg/kg corresponded to a rate of 0.5 kg of heptenophos/ha in the field. Radiochemical procedures were used to monitor the breakdown.

**Role of Microorganisms.** Comparison of radioactivity distribution in the different fractions of microbially active (Table 2) and sterile soil (data not shown) shows that the portion of nonextractable residue is increased by microbial activity. In addition, degradation by microorganisms leads to formation of $^{14}CO_2$, which was not produced in sterile soils. High amounts of extractable radioactivity were obtained with sterile soil. The increased persistence of heptenophos in autoclaved soil illustrates the role of microorganisms in its degradation. In microbially active soil, heptenophos is rapidly degraded into three principal and four minor compounds. In autoclaved soil, transformation products were not formed until hour 168. The formation of metabolites 1 and 2 in sterile soil can be explained by a small number of aerobic bacteria detected at the end of the incubation (data not shown). Aerobic bacteria form heat-resistant spores which can survive the sterilization process (Schlegel, 1981). During the incubation, the spores germinate and lead to the formation of the primary degradation products, metabolites 1 and 2. This implies that under these conditions, heptenophos is degraded predominantly by microbial action. The persistence of heptenophos in autoclaved soil indicates that chemical hydrolysis is a minor factor.

**Biological Baeyer–Villiger Oxidation.** On the basis of the present results, a degradation scheme was proposed which is presented in Figure 6. Starting with heptenophos, metabolite 1 is produced by ester hydrolysis and subsequent keto–enol tautomerization (Lehmann, 1972). The further degradation can be best described as a biological Baeyer–Villiger oxidation first suggested by Trudgill (1984). This ring oxygen insertion has been shown to be mediated by ketone 1,2-monooxygenases and has been observed in plant and microorganism metabolism. Although the Baeyer–Villiger reaction is well known for the degradation of biologically formed substances, e.g., *l*-menthone, camphor (Croteau, 1987), *d*-fenchone (Chapman et al., 1965), and simple cyclic ketones (Trudgill, 1984; Alphand et al., 1989), metabolites 2 and 4 appear to be the first pesticide metabolites formed by biological Baeyer–Villiger oxidation. The formation of metabolite 2 is explainable by Baeyer–Villiger oxidation of metabolite 1, whereas metabolite 4 might be formed by Baeyer–Villiger oxidation via postulated intermediate 8 or 9. Surprisingly, the oxygen is inserted into the ring system at different positions by both biological Baeyer–Villiger oxidations. In contrast, chemical synthesis always yielded compounds 2 and 10 as major products. So far we have no explanation for the different selectivity of both biological oxidations. The generation of metabolite 5 is more complex and may be due either to lactone cleavage of metabolite 2, oxidation of the formed alcohol and elimination of hydrogen chloride, or to lactone cleavage of 10, oxidation of the formed alcohol and dehydrogenation. Finally, the metabolites are incorporated into nonextractable residues or further degraded to $CO_2$.

In summary, the degradation of heptenophos in this soil environment is a result of microbiological processes. The main reaction after hydrolysis of the phosphate ester is a biological Baeyer–Villiger oxidation converting the stable cyclic ketones into unstable lactones which may be hydrolyzed with the formation of substituted carboxylic acids.

## ACKNOWLEDGMENT

We extend appreciation to Frank Zurmühlen for synthesizing standards of metabolites 2 and 4 and thank Michael Gübert for GC/MS analyses and Eduard Zeisberger for GC/FTIR analyses.

## LITERATURE CITED

Alphand, V.; Archelas, A.; Furstoss, R. Microbial Transformations 16. One-step Synthesis of a Pivotal Prostaglandin Chiral Synthon via a Highly Enantioselective Microbiological Baeyer-Villiger Type Reaction. *Tetrahedron Lett.* **1989**, *30*, 3663–3664.

Bonin, W. Heptenophos, a new insecticide for the control of ectoparasites. *Proc. Br. Insectic. Fungic. Conf. 8th* **1975**, 2, 705–709.

Chapman, P. J.; Meerman, G.; Gunsalus, I. C. The microbiological transformation of fenchone. *Biochem. Biophys. Res. Commun.* **1965**, *20*, 104–108.

Croteau, R. Biosynthesis and catabolism of monoterpenoids. *Chem. Rev.* **1987**, *87*, 929–954.

Emmel, L.; Gorbach, S.; Mildenberger, H.; Röchling, H.; Vulic, M. Hoe2982, Systemic phosphoric ester with short persistence. *Summaries of Papers. VII*, International Congress Plant Protection, Paris, 1970, p 125.

Hewson, R. T. Heptenophos, a new systemic insecticide of short persistence. *Proc. Br. Insectic. Fungic. Conf. 8th* **1975**, *2*, 697–704.

Lehmann, P. Heptenophos-14-C, Elimination via urine and faeces. Ph.D. Dissertation, The University of Mainz, Germany, 1972.

Matsumoto, M.; Kobayashi, H. Oxidation of Cyclobutanones to γ-Butyrolactones with Hydrogen Peroxide in 2,2,2-Trifluoroethanol. *Heterocycles* **1986**, *24*, 2443–2447.

Schlegel, H. G. *Allgemeine Mikrobiologie*; Thieme: Stuttgart, Germany, 1981.

Timme, G.; Frehse, H. Zur statistischen Interpretation und graphischen Darstellung des Abbauverhaltens von Pflanzenbehandlungsmittel-Rückständen. I. Statistical interpretation and graphic representation of the degradational behavior of pesticide residues. I. *Pflanzenschutz-Nachr Bayer* **1980**, *33*, 47–60.

Timme, G.; Frehse, H.; Laska, V. Zur statistischen Interpretation und graphischen Darstellung des Abbauverhaltens von Pflanzenschutzmittel-Rückständen. II. Statistical interpretation and graphic representation of the degradational behavior of pesticide residues. II. *Pflanzenschutz-Nachr. Bayer* **1986**, *39*, 188–204.

Trudgill, P. W. Microbial degradation of the alicyclic ring, Structural relationships and metabolic pathways. In *Microbial degradation of organic compounds*; Gibson, D. T., Ed.; Dekker: New York 1984; pp 131–180.

Received for review December 27, 1993. Accepted April 14, 1994.[⊗]

[⊗] Abstract published in *Advance ACS Abstracts,* June 1, 1994.